

Liquid-gas binodal anomaly for systems with pairing transition

 H. Stein^{1,a}, C. Porthun², and G. Röpke¹
¹ Fachbereich Physik, Universität Rostock, Universitätsplatz 3, 18051 Rostock, Germany

² Alfred-Wegener-Institut für Polar- und Meeresforschung, 27568 Bremerhaven, Germany

Received: 14 October 1997 / Accepted: 2 December 1997

Abstract. For fermionic model systems with a separable interaction the BCS equations are solved self-consistently. In addition, the possibility of a liquid-gas phase transition is considered by inspecting thermodynamic stability. Different examples of temperature-density phase diagrams are given depending on the parameters of a model interaction. In particular, a liquid-gas binodal anomaly is found due to the superposition of the superfluid and the liquid-gas phase transition.

PACS. 05.30.Fk Fermion systems and electron gas – 64.70.Fx Liquid-vapor transitions – 67.20.+k Quantum effects on the structure and dynamics of nondegenerate fluids (e.g., normal phase liquid ⁴He)

1 Introduction

An interesting phenomenon in interacting fermion systems is pairing, which leads to a superfluid phase transition. If the attractive part of the interaction is strong enough to form a bound state in the low density limit, a crossover from Bose-Einstein condensation (BEC) at low densities to BCS pairing at high densities is expected to occur (for an overview of relevant systems see [1]). There are different systems in condensed matter physics, *e.g.*, the electron-hole system in excited semiconductors where such a crossover may occur [2,3]. Symmetric nuclear matter is a particular example of a strongly coupled quantum liquid with a crossover from BEC to BCS pairing [4,5].

However, homogeneous solutions of the equation of state including the transition to superfluidity have to be excluded if the condition of phase stability is violated. The corresponding instability leads to a liquid-gas phase transition which is connected with a jump of the density at given temperature. Therefore, an interesting question is whether the pairing transition, which may occur at low temperatures in an interacting fermion system, can be realized in thermodynamic equilibrium.

For instance, in symmetric nuclear matter the pairing transition [6] is hidden to a large extent by the nuclear matter liquid-gas phase transition [7,8]. Nevertheless, effects of pairing are observable in finite systems (nuclei, see [9]) or in asymmetric nuclear matter (neutron stars, see [10]).

In the present paper we show how the ordinary liquid-gas transition in a normal system is influenced by a pairing

transition. A main objective is the study of the modification of the instability region in the temperature-density plane. We consider a model system with a general form of the interaction that allows us to explore different types of phase diagrams, depending on the overlap between the liquid-gas phase coexistence area and the superfluid phase, and draw some conclusions for thermodynamic properties.

2 Pairing and thermodynamic stability

Standard BCS theory [11] describes superconductivity as well as superfluidity in fermionic systems by the formation of Cooper pairs as a result of an effective attraction. The variational Hamiltonian with fermion creation and annihilation operators a_1^\dagger and a_1 reads

$$\begin{aligned}
 H = & \sum_1 \left(\frac{k_1^2}{2m} - \mu \right) a_1^\dagger a_1 \\
 & + \frac{1}{2} \sum_{1,2,1',2'} V(12,1'2') a_1^\dagger a_2^\dagger a_{2'} a_{1'}.
 \end{aligned}
 \tag{1}$$

The indices denote quantum numbers such as momentum and spin: $1 = \{k_1, \sigma_1\}$ or $\bar{1} = \{-k_1, -\sigma_1\}$.

Here, the set of self-consistent BCS equations at finite temperature is reviewed from a thermodynamic Green's functions approach using a pair cut-off procedure to decouple higher order correlations [8]. For convenience, the reduced Planck constant \hbar and the Boltzmann constant k_B are omitted in the following.

The single particle energy ε_1 in the grand canonical ensemble contains the selfenergy Σ in BCS meanfield

^a e-mail: holger@darss.mpg.uni-rostock.de

approximation

$$\varepsilon_1 = \frac{k_1^2}{2m} - \mu + \text{Re} \Sigma^{BCS}(1), \quad (2)$$

$$\text{Re} \Sigma^{BCS}(1) = \sum_2 [V(12, 12) - V(12, 21)] \langle a_2^\dagger a_2 \rangle. \quad (3)$$

The mean occupation number of a single fermion state $|1\rangle$ is given by

$$\langle a_1^\dagger a_1 \rangle = \frac{1}{2} - \frac{\varepsilon_1}{2\sqrt{\varepsilon_1^2 + \Delta^2(1)}} \tanh \left[\frac{\sqrt{\varepsilon_1^2 + \Delta^2(1)}}{2T} \right]. \quad (4)$$

The gap function, $\Delta(1)$, is given by the equation

$$\Delta(1) = - \sum_2 \frac{V(1\bar{1}, 2\bar{2}) \Delta(2)}{2\sqrt{\varepsilon_2^2 + \Delta^2(2)}} \tanh \left[\frac{\sqrt{\varepsilon_2^2 + \Delta^2(2)}}{2T} \right]. \quad (5)$$

The Dyson equation (3) for the single particle self energy, the mean occupation number equation (4) and the gap equation (5) represent a set of equations that must be solved simultaneously at given temperature.

Above a critical temperature for the onset of pairing, T_{BCS} , this set of equations has only the solution with vanishing gap $\Delta(1) = 0$. This is equivalent to the Hartree-Fock (HF) mean field solution. For this case the mean occupation number in equation (4) coincides with the Fermi distribution function

$$\langle a_1^\dagger a_1 \rangle = (\exp[\varepsilon_1/T] + 1)^{-1} \quad \text{for } T \geq T_{BCS}. \quad (6)$$

Below T_{BCS} a solution with $\Delta(1) = 0$ and another solution with $\Delta(1) \neq 0$ exist. Only the latter one is stable and characterizes the superfluid phase.

Summing up the mean occupation numbers, equation (4), a relation between chemical potential, temperature and single particle density follows:

$$n(T, \mu) = \frac{1}{V} \sum_1 \langle a_1^\dagger a_1 \rangle. \quad (7)$$

However, this equation can only be considered as an equation of state if the criterion of thermodynamic stability is fulfilled.

In general, a thermodynamically stable system in equilibrium is given by a minimum of the grand canonical potential $\Omega(T, V, \mu)$, that can be obtained by means of equation (7)

$$\Omega(T, V, \mu) = V \int_{-\infty}^{\mu} d\mu' n(T, \mu'). \quad (8)$$

Correspondingly, the condition for thermodynamic stability is

$$\left. \frac{\partial \mu}{\partial n} \right|_T \geq 0. \quad (9)$$

The violation of this condition is a signature of a first order phase transition. It can be caused by an attractive two-particle interaction. The respective instability region separates the stable phases, which in the following are denoted as the gas and the liquid phase. The coexistence region of both phases is determined from a Maxwell construction. Its envelope is denoted as the binodal.

3 Results for systems with separable interaction

In our exploratory calculation for a fermion system the interaction $V(12, 1'2')$ is modeled by a separable potential that has advantageous analytic properties. According to the method of Ernst, Shakin and Thaler [12] any given potential can be represented by a series of separable potentials. In each scattering channel α the interaction can be parametrized by a potential $V_\alpha(k, k')$ of rank N which is separable in the incoming, $k = (k_1 - k_2)/2$, and outgoing, $k' = (k_{1'} - k_{2'})/2$, relative momenta

$$\begin{aligned} V_\alpha \left(\frac{K}{2} + k, \frac{K}{2} - k, \frac{K'}{2} + k', \frac{K'}{2} - k' \right) &= V_\alpha(k, k') \delta_{KK'} \\ &= \sum_{i,j=1}^N v_{\alpha i}(k) \lambda_{\alpha ij} v_{\alpha j}(k'). \end{aligned} \quad (10)$$

It does not depend on the total momentum $K = k_1 + k_2$. This kind of potential is frequently used in nuclear physics to model the nucleon-nucleon interaction (*e.g.*, [13,14]) or semiconductor physics for the electron-hole interaction (*e.g.*, [2]). It allows the explicit solution of the Schrödinger equation as well as for the T -matrix in the formalism of thermodynamic Green's functions.

An implicit expression for the gap energy follows from equation (5) for each (uncoupled) scattering channel

$$1 = - \int \frac{dk^3}{(2\pi)^3} \frac{V(k, k)}{2\sqrt{\varepsilon_k^2 + \Delta^2(k)}} \tanh \left[\frac{\sqrt{\varepsilon_k^2 + \Delta^2(k)}}{2T} \right]. \quad (11)$$

For vanishing gap energy the Thouless criterion for the onset of pairing [15] results (equivalent to the pole condition of the thermodynamic two-particle T -matrix, $T(kK, k'K'; E)$, at zero total momentum and two-particle energy $E = 2\mu$ [4])

$$1 = - \int \frac{dk^3}{(2\pi)^3} \frac{V(k, k)}{2\varepsilon_k} \tanh \left(\frac{\varepsilon_k}{2T_{BCS}} \right). \quad (12)$$

For a strong-enough interaction bound state formation may occur. The bound state energy, $E(K)$, can be determined from the pole in the two-particle T -matrix $T(kK, k'K'; E)$. The bound state merges with the continuum of scattering states if $E(K) = K^2/4m + 2\text{Re} \Sigma^{BCS}(K/2)$. The disappearance of the pole in the two-particle T -matrix for total momentum $K = 0$ is equivalent to the Mott condition where bound states are dissolved due to the Pauli-blocking in the system [4]

$$\begin{aligned} 1 &= - \int \frac{dk^3}{(2\pi)^3} \frac{V(k, k)}{k^2/m + 2\text{Re} \Sigma^{BCS}(k) - 2\text{Re} \Sigma^{BCS}(0)} \\ &\quad \times \tanh \left(\frac{\varepsilon_k}{2T_{Mott}} \right). \end{aligned} \quad (13)$$

In the following, we present results of numerical calculations with different potential parameter sets in the s -wave

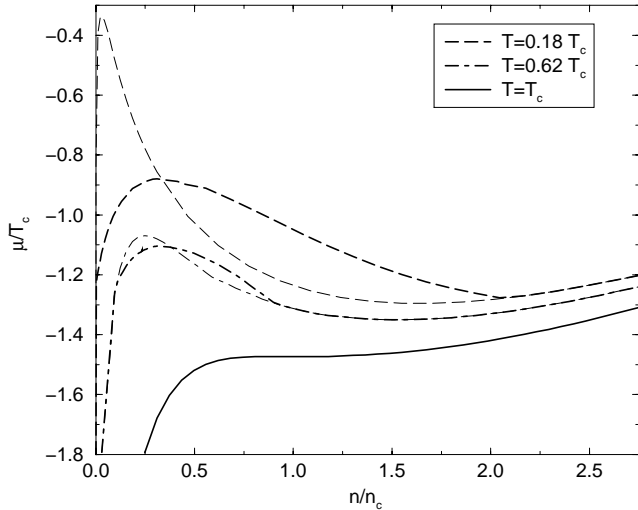


Fig. 1. Isotherms of chemical potential *versus* density (interaction with rank 1 potential and inverse potential range $a = 0.4$). Bold lines represent the stable BCS solution with finite gap below T_{BCS} , thin lines the unstable solution with zero gap.

channel for a fermion system that shows both, a superfluid and a liquid-gas phase transition. We do not focus on a particular system. Instead, we want to study in an exploratory calculation systems that are expected to show some effects due to the interplay of both transitions.

3.1 Model calculation with pure attractive interaction

To explore possible effects of the interplay of both transitions, we start with the most simple case of a separable potential of rank 1. It has only an attractive term: $V(k, k') = -v(k)v(k')$ with a form factor $v(k) = c(k^2 + a^2)^{-1}$, where c and a are potential strength and range parameters. We consider a strongly interacting system where bound states can be formed. Solving the Schrödinger equation with this potential one obtains the binding energy E_b^0 and can eliminate the potential strength parameter c . Thus, any quantity in our formulae can be represented as a combination of energy units measured in $|E_b^0|$ and length units measured in $\hbar/\sqrt{m|E_b^0|}$. Then the potential strength can be expressed by $c^2 = 8\pi a(a+1)^2$ and the inverse potential range, a , remains the only (dimensionless) parameter. Variation of this parameter leads to situations with different overlaps of the liquid-gas instability and the superfluid region. The resulting effects can be compared systematically. A system with such an interaction potential and spin-degeneracy 2 (fermions with spin $\pm 1/2$) shows no liquid-gas transition if the potential range is too short ($a > 1$) while the superfluid phase remains. For better comparison the quantities in all figures are plotted in units of the critical temperature T_c and the critical density n_c of the liquid-gas phase transition (reduced units).

Figures 1 and 2 result from the self-consistent solution of equations (3-5, 7) for the rank 1 potential with inverse potential range $a = 0.4$. In Figure 1 isotherms of the solu-

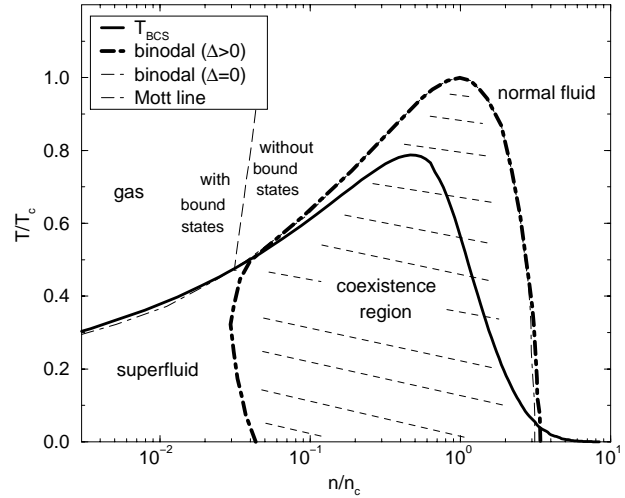


Fig. 2. Phase diagram in the temperature-density plane for a fermion system with rank 1 potential and inverse potential range $a = 0.4$. The liquid-gas coexistence region resulting from the stable BCS solution (bold dashed-dotted) is compared to the unstable solution (thin dashed-dotted) with vanishing gap. The full bold line shows the onset of pairing at temperature $T_{BCS}(n)$ according to equation (12). Its maximum is below the critical temperature T_c for the liquid-gas transition. The dashed Mott line is obtained from equation (13) and shows where bound states start to break up at higher densities due to Pauli-blocking.

tions with finite gap and with zero gap are compared. Both kinds of isotherms show a thermodynamic instability if the temperature is lower than the critical temperature T_c of the liquid-gas transition. Above the maximum temperature for the onset of pairing $T_{BCS} = 0.8T_c$ only the zero gap solution (HF solution) remains. Figure 2 shows the resulting temperature-density phase diagram after application of the Maxwell construction to the isotherms $\mu(n, T)$. The coexistence region determined from the BCS equations with finite gap has shrunk if compared to the zero gap solution. This effect of binodal anomaly is clearly obtained for temperatures below the point of intersection between the binodal and the critical temperature for the onset of pairing.

Figure 3 shows the phase diagram for a system with shorter potential range ($a = 0.6$). This particular case shows an even more distinct coexistence anomaly. Here, the interaction leads to a superfluid phase that completely encloses the liquid-gas instability region. Hence, the full BCS mean field solution deviates strongly from the HF solution. Even the critical point is shifted to higher temperatures and densities while the coexistence region forms an island-like structure. The strong influence of the gap on the renormalization of the chemical potential destroys the instability if the temperature approaches zero.

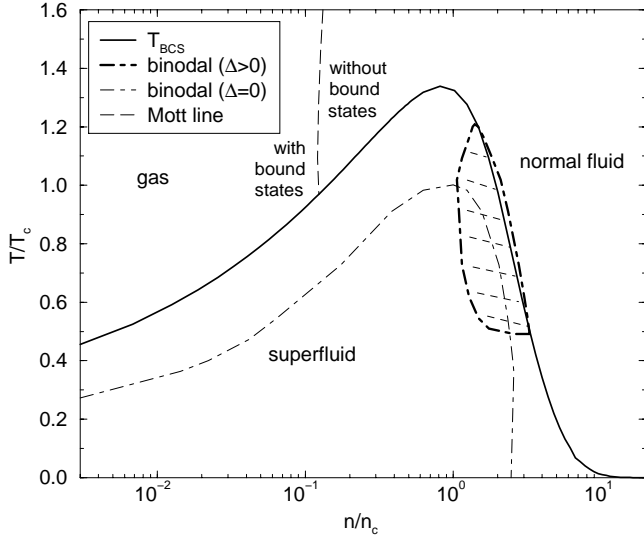


Fig. 3. Phase diagram in the temperature-density plane for a fermion system with rank 1 potential and inverse potential range $a = 0.6$. In contrast to the (unstable) solution with vanishing gap (thin dashed-dotted), the liquid-gas coexistence region resulting from the stable solution with finite gap (bold dashed-dotted) has shrunk to an island-like area. The full bold line shows the onset of pairing at temperature $T_{BCS}(n)$ according to equation (12). Its maximum is above the critical temperature T_c . The dashed Mott line, equation (13), shows where bound states start to break up at higher densities due to Pauli-blocking.

3.2 Model calculation with attractive and repulsive interaction

In a next step we employ a more general separable potential including an attractive tail and a repulsive core. That allows us to explore a larger variety of possible types of phase diagram. For sake of simplicity, we have used a separable potential of rank 2 which has a long range attraction term (index “ a ”) and short range repulsion term (index “ r ”), each of them with one range and one strength parameter

$$V(k, k') = v_r(k)v_r(k') - v_a(k)v_a(k') \quad (14)$$

with

$$v_i(k) = c_i(k^2 + a_i^2)^{-1}, \quad i = \{r, a\}.$$

This type of potential was used for the parametrization of the nucleon-nucleon interaction [14]. It represents the fact that, besides a long range attraction, a short range repulsion is necessary to reproduce such two-particle properties as the nucleon-nucleon scattering phase shifts. One of the parameter sets for the 3S_1 partial wave (neutron-proton scattering) presented in [14] is $a_r = 4.54 \text{ fm}^{-1}$, $c_r = 566.0 \sqrt{\text{MeV}/\text{fm}}$, $a_a = 1.908 \text{ fm}^{-1}$ and $c_a = 155.6 \sqrt{\text{MeV}/\text{fm}}$. Note that the strength parameters given in [14] already contain a factor $(2\pi^2)^{-1}$. With the nucleon mass a constant $\hbar^2/m = 41.46 \text{ MeVfm}^2$ is used. For nuclear matter, the influence of the superfluid phase on the liquid-gas coexistence region is not significant since

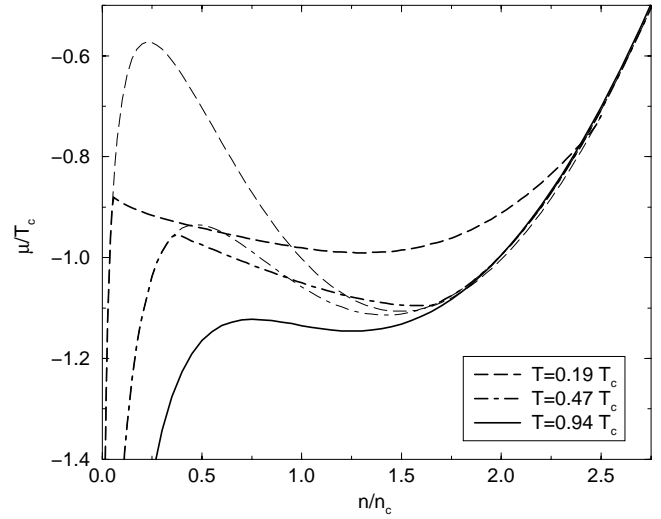


Fig. 4. Isotherms of chemical potential *versus* density according to equation (7) for a system with the interaction in equation (14). Bold lines show the stable BCS mean field solution with non-vanishing gap below T_{BCS} , thin lines represent the unstable solution with vanishing gap (reduced units).

the superfluid transition region is well below and covered by the liquid-gas instability [8].

In our model calculation we have chosen a rank 2 potential with arbitrary parameters which not necessarily refer to the particular case of a nucleon-nucleon interaction. To highlight the effect of the interplay between the superfluid and the liquid-gas transition we have used the following parameter-set for the potential in equation (14) $a_r = 2.934 \text{ fm}^{-1}$, $c_r = 770.4 \sqrt{\text{MeV}/\text{fm}}$, $a_a = 1.908 \text{ fm}^{-1}$ and $c_a = 355.4 \sqrt{\text{MeV}/\text{fm}}$. The results of the self-consistent solution of the set of equations (3-5, 7) for a system with spin degeneracy 4 (*e.g.*, with spin and isospin) are shown in Figures 4 and 5. A significant difference between the renormalization of the chemical potential for a finite gap solution and for a zero gap solution inside the superfluid phase is obtained (see Fig. 4). In the finite gap solution a sharp cusp occurs at densities where superfluidity sets in. This behaviour is typical for a second order phase transition, for which the first derivative of the thermodynamic potential is continuous but not differentiable. In addition, a liquid-gas instability occurs for both kinds of solutions. Both solutions coincide above the maximum critical temperature for superfluidity, $T_{BCS} = 0.85T_c$.

Figure 5 follows like Figure 5 after application of the Maxwell construction to the isotherms $\mu(n, T)$. It shows a situation where the superfluid phase is not hidden by the liquid-gas instability region for higher densities. The point, where the normal liquid, the superfluid and the instability region meet together, has a temperature of about $0.64T_c$. In the following, this point is denoted analogous to the corresponding point in the helium phase diagram (see discussion below) as λ -point. Here, its value is the same order of magnitude as the maximum critical temperature for the onset of pairing $T_{BCS} = 0.85T_c$. Compared to the

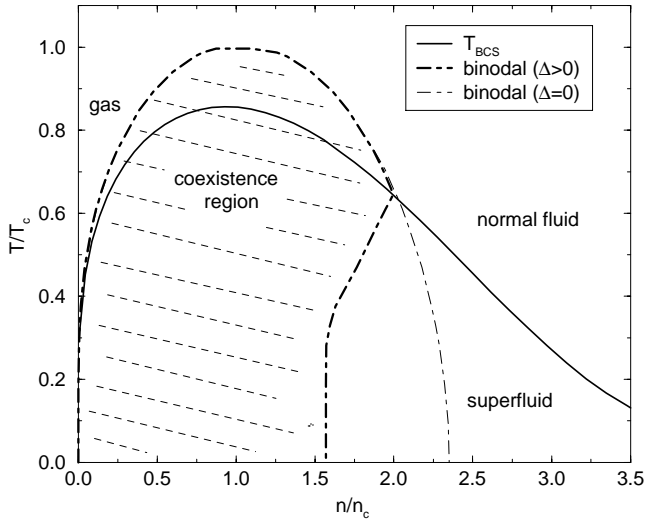


Fig. 5. Phase diagram in the temperature-density plane for the same system as in Figure 4. The liquid-gas coexistence region resulting from the stable BCS solution (bold dashed-dotted) is compared to unstable solution (thin dashed-dotted) with vanishing gap. The full bold line shows the onset of pairing at temperature $T_{BCS}(n)$, according to equation (12) (reduced units).

unstable solution with vanishing gap the area of the liquid-gas coexistence region is clearly reduced in the case of the stable BCS solution.

4 Discussion

We have considered phase diagrams of strongly interacting fermion systems showing both liquid-gas and superfluidity transitions. Examples with a rank 1 separable interaction are presented. To cover a richer variety of phase diagrams we have also considered a rank 2 separable interaction potential. For a special set of parameters we modeled a phase diagram where the critical point of the liquid-gas transition and the λ -point (point of intersection between binodal and superfluid transition temperature) are of the same order of magnitude. Then an essential deformation of the binodal near the λ -point is obtained, which is denoted as binodal anomaly. If the coexistence region determined for vanishing gap energy is completely covered by the superfluid phase, as shown in Figure 3, the binodal derived from the stable BCS solution is changed completely. We do not know whether systems of this type occur in nature.

Symmetric nuclear matter is an example of a fermionic system that is known to exhibit a liquid-gas and a superfluid phase transition [4, 8]. However, the influence of the superfluid region on the shape of the liquid-gas instability is negligibly small since it is almost completely hidden by the latter and the critical liquid-gas temperature (about 15-20 MeV) is much higher than the point of intersection between the binodal and the critical BCS temperature, which occurs below 1 MeV.

In asymmetric nuclear matter the liquid-gas transition region is suppressed [16]. Singlet pairing (neutron-neutron)

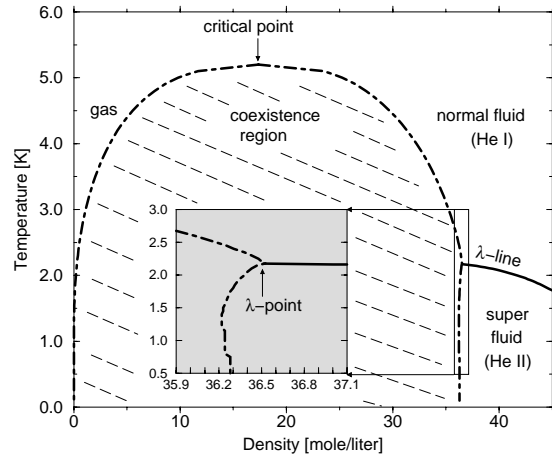


Fig. 6. Temperature-density diagram for ${}^4\text{He}$ showing different stable phases and the coexistence region limited by the binodal, which separates liquid and gas phases (data taken from [17]). The critical point is $T_c = 5.25$ K, $n_c = 17.3$ mol/l and $p_c = 2275$ hPa. Inset: enlarged view near the λ -point ($T_\lambda = 2.17$ K, $n_\lambda = 36.5$ mol/l and $p_\lambda = 50.35$ hPa).

becomes more important than triplet pairing (proton-neutron). For this case, the effect of the binodal anomaly could become important.

For a further discussion of interacting fermion systems with strong coupling the possible formation of bound states has to be taken into account. It becomes important for the thermodynamic properties of the system at densities below the Mott-density (see Mott-line in Figs. 2 and 3). The bosonic bound states can undergo Bose-Einstein condensation. For an appropriate description one must apply a theory that goes beyond the BCS mean field approximation. One attempt at a better description of the normal phase is given by Nozières and Schmitt-Rink [2] where the correlations are explicitly considered as additional contributions in the equation of state. In a generalized approach (generalized Beth-Uhlenbeck formula) this method has been applied to the case of nuclear matter in the normal phase [4, 5]. An extension of the method to the superfluid phase is still lacking.

Finally, we want to focus the readers attention on a real bosonic system that exhibits a binodal anomaly of the type discussed above. Helium-4 is an extensively investigated example that shows both a first order liquid-gas phase transition and a superfluid phase transition (see binodal and λ -line in Fig. 6).

It is the only substance known to us having a superfluid transition temperature, $T_\lambda = 2.17$ K, in the same order as the temperature of the critical point, $T_c = 5.25$ K. (The fermionic isotope helium-3 with $T_c = 3.34$ K shows superfluidity only at temperatures below 2.7 mK.) We have plotted the helium-4 data [17] of the interesting region in a temperature-density phase diagram (see Fig. 6). It shows the stable phases, gas and liquid (normal HeI and superfluid HeII), separated by the coexistence region. The inset is an enlarged view of the region around the λ -point. While

the liquid-gas coexistence curve (binodal) decreases monotonically with negative slope above the critical density, it bends back at the λ -point and even has a positive slope for lower temperatures. This is the phenomenon which we have described above as a liquid-gas binodal anomaly.

We expect that the binodal anomaly can occur in Bose systems as well as in Fermi systems in case of an appropriate overlap of the liquid-gas instability region and the superfluid region. Thus, the effects should also be studied for interacting Bose systems. The last few years have seen a renewal of interest in the phenomenon of phase transitions in Bose systems, from both experimental and theoretical (for an overview [1,18]); especially since the first atomic Bose condensates have been produced [19]. While the possibility of single-boson BEC is extensively discussed for dilute systems, it is known that interacting Bose systems can show a transition analogous to the BCS transition [20]. This type of bosonic pairing has been investigated for a wide range of systems, such as pion gases [22] and atomic gases like ${}^7\text{Li}$ [21].

5 Conclusion

We have considered the phase stability of a fermion system with respect to a liquid-gas phase transition. Compared to the solution for vanishing gap energy we have shown that due to the occurrence of a superfluid phase a deformation of the coexistence region results. This effect of the liquid-gas binodal anomaly becomes stronger if the coexistence region and the superfluid phase overlap in such a way that the point of intersection between the binodal and the critical temperature for the onset of superfluidity (λ -point) is closer to the critical point. For this reason the effect is negligibly small in symmetric nuclear matter. However, it could be important in other systems, such as asymmetric nuclear matter or electron-hole liquids with excitonic molecules in semiconductors. For the latter case the possible types of phase diagrams are drawn schematically in [23] showing a binodal anomaly in agreement with our discussion.

Our calculations are carried out in a self-consistent mean field approximation for the gap equation. Interacting fermion systems with strong coupling can show the formation of bosonic bound states (*e.g.* deuterons and α -particles, excitons and bi-excitons), which can undergo Bose-Einstein condensation. For an appropriate description of strong correlations the interaction between bound states has to be considered in a consistent way. The improvement of the self-consistent mean field approach by including strong correlations is an important point of future work (attempts can be found in [3,24]).

As a fermionic example we have discussed nuclear matter. The effect of the liquid-gas binodal anomaly

is also expected to occur in Bose systems. An example of relevance would be a microscopic description of the behaviour of helium-4 in the vicinity of its λ -point.

We thank Peter Schuck for reading and discussing the manuscript.

References

1. *Bose-Einstein Condensation*, edited by A. Griffin, D.W. Snoke, S. Stringari (Cambridge University Press, Cambridge, 1995).
2. P. Nozières, S. Schmitt-Rink, *J. Low Temp. Phys.* **59**, 195 (1985).
3. G. Röpke, *Ann. Physik (Leipzig)* **3**, 145 (1994); G. Röpke, *Z. Phys. B* **99**, 83 (1995).
4. M. Schmidt, G. Röpke, H. Schulz, *Ann. Phys. (N.Y.)* **202**, 57 (1990).
5. H. Stein, A. Schnell, T. Alm, G. Röpke, *Z. Phys. A* **351**, 295 (1995).
6. P. Ring, P. Schuck, *The Nuclear Many-Body Problem* (Springer, Berlin, 1980).
7. G. Röpke, M. Schmidt, L. Münchow, H. Schulz, H., *Nucl. Phys. A* **379**, 536 (1982) **A 399**, 587 (1983).
8. R.K. Su, S.D. Yang, T.T.S. Kuo, *Phys. Rev. C* **35**, 1539 (1987).
9. A. Bohr, B.R. Mottelson, *Nuclear Structure*, Vol. I (Benjamin, New York, 1969).
10. S.L. Shapiro, S.A. Teukolsky, *Black Holes, White Dwarfs and Neutron Stars* (Wiley, New York, 1983).
11. J. Bardeen, L.N. Cooper, J.R. Schrieffer, *Phys. Rev.* **108**, 1175 (1957).
12. D.J. Ernst, C.M. Shakin, R.M. Thaler, *Phys. Rev. C* **8**, 46 (1973).
13. Y. Yamaguchi, *Phys. Rev.* **95**, 1628 (1954).
14. T.R. Mongan, *Phys. Rev.* **175**, 1260 (1968); *Phys. Rev.* **178**, 1597 (1969).
15. D.J. Thouless, *Ann. Phys. (NY)* **10**, 553 (1960).
16. H. Müller, B.D. Serot, *Phys. Rev. C* **52**, 2072 (1995).
17. R.D. McCarty, *J. Phys. Chem. Ref. Data*, Vol 2, No. 4 (1973); R.D. McCarty, NBS TN 1024 (1980).
18. *J. Res. Natl. Inst. Stand. Technol.*, **101** (1996).
19. M.H. Anderson, J.R. Ensher, M.R. Matthews, C.E. Wieman, E.A. Cornell, *Science* **269**, 198 (1995); C.C. Bradley, C.A. Sackett, J.J. Tollett, R.G. Hulet, *Phys. Rev. Lett.* **75**, 1687 (1995); K.B. Davis, M.-O. Mewes, M.R. Andrews, N.J. van Druten, D.S. Durfee, D.M. Kurn, W. Ketterle, *Phys. Rev. Lett.* **75**, 3969 (1995).
20. W.B. Evans, Y. Imry, *Nuovo Cimento B* **63**, 155 (1969); W.B. Evans, R.I.M.A. Rashid, *J. Low. Temp. Phys.* **11**, 93 (1973).
21. H.T.C. Stoof, *Phys. Rev. A* **49**, 3824 (1994).
22. T. Alm, G. Chanfray, P. Schuck, G. Welke, *Nucl. Phys. A* **612**, 472 (1997).
23. L.V. Keldysh, contribution in [1], 246.
24. R. Haussmann, *Z. Phys. B* **91**, 291 (1993).